ComplexBRAT: Complex Backward Reach-Avoid Tubes. An Emergent Collective Behavior Framework.

Olalekan Ogunmolu

Microsoft Research, NYC, 300 Lafayette Street, New York, NY 10012, USA
lekanmolu@microsoft.com.

Abstract. We are concerned with finding control laws with input and state constraints-satisfaction guarantees in nonlinear multi-agent systems that exhibit complex dynamics. Therefore, we present a scheme for constructing backward reach-avoid-tubes (BRATs) which return safety certificates or guarantees for such systems. We locally resolve the extremal of payoffs for separated local subsystems and prescribe a numerical scheme to assemble these local BRATs. Within the bounds here set, our scheme presents a simple yet effective strategy for designing the verification of *complex nonlinear systems* via backward reach-avoid sets or tubes.

1 INTRODUCTION

This, in essence, is the problem that we address: computing control laws in the presence of input and state constraints in large-scale (complex) nonlinear systems. In the rest of this document, we shall present a scheme for locally computing "safety-preserving" *backward reach-avoid tubes* (BRATs) [1–3]. BRATs are those zero-level sets [4] of implicitly-defined value functions on a state space that return a "safety-satisfying" certificate after solving a Cauchy-type Hamilton-Jacobi Isaacs equation [5, 6]. Throughout, we shall work under a uniform dynamics property among all agents and the property that local and global kinematics are driven by external disturbances. We shall then prescribe an aggregation scheme for prescribing a global constraints-satisfaction guarantee in such systems.

Applications of these methods may include (i) the robust coordination of the motion of search and rescue robot-teams in a complex terrain; (ii) motion-planning under state and input constraints for human-robot interactive systems e.g. in warehouse assembly operations; (iii) coordinating system operation based on a labyrinth of sensor nodes replete throughout a vectogram in life-critical internet of medical things (IoMT); (iv) energy efficiency control and management in large buildings where end-user demand-response must be accurately predicted for evaluating fixed rule strategies and control actions, *inter alia*.

Differential optimal control theory and games offer a useful paradigm for resolving the backward reach-avoid tubes (BRAT) of multiple agents interacting over a large shared space. Both rely on the resolution of the Hamilton-Jacobi-Bellman (HJB) equation or its Isaacs counterpart (HJI). As HJ-type equations are seldom regular enough to admit a classical solution for almost all *practical* problems, "weaker" or "viscosity" solutions [5,

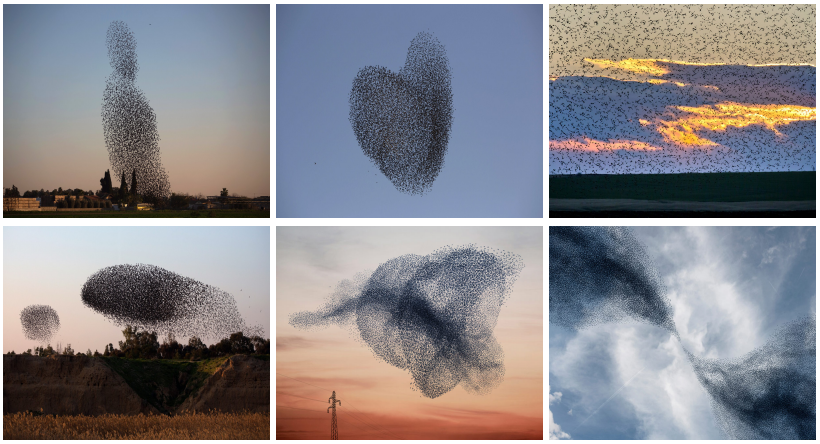

Fig. 1: Starlings murmurations. From the top-left and clockwise. (i) A starlings flock rises into the air, in a dense structure (Reuters/Amir Cohen). (ii) Starlings migrating over an Israeli village (AP Photo/Oded Balilty). (iii) Starlings feeding on laid seeds in the ground in Romania. (iv) Two flocks of migrating starlings (Menahem Kahana/AFP/Getty Images). (v) A concentric conical formation of starlings (Courtesy of The Gathering Site.). (vi) Splitting and joining of a flock of starlings.

7, 8] provide generalized solutions to HJ partial differential equations (P.D.E.s) under relaxed regularity conditions; these viscosity solutions are not necessarily differentiable anywhere in the state space, and the only regularity prerequisite in the definition is continuity [6]. However, wherever they are differentiable, they satisfy the values of HJ P.D.E.s in a classical sense. Thus, they lend themselves well to many real-world problems existing at the interface of discrete, continuous, and hybrid systems [2, 3, 9, 10].

With the elegant theoretical results of [5, 8, 11–13], stable essentially non-oscillatory Lax-Friedrichs numerical integration schemes provide *consistent* and *monotone* viscosity solutions with high accuracy and precision *on a mesh* to multi-dimensional HJ-type equations[1]. However, by discretizing the Hamiltonian on a dimension-by-dimension basis, the scheme suffers from scalability as a result of the exponential computational complexity associated with grid resolutions of value functions [14–16]. Given the limits of computational resources and memory when resolving practical problems for multiagent systems, what if we exploit local structures within a complex system and resolve the overall Hamiltonian by an aggregation of the computation of the numerical fluxes of local Hamiltonians? This is the central question that this paper seeks to address.

For many natural systems such as multiple agent systems, foaming across scales, multicellular structures, crystallography e.t.c, the interconnection among subsystems can be characterized as moving interfaces which are boundaries of interacting local regions

[1] Consistent solutions to HJ equations are those whose explicit marching schemes via discrete approximations to the HJ IVP agree with the nonlinear HJ solution [12]. Such schemes are said to be *monotone* e.g. on $[-\mathbb{R}, \mathbb{R}]$ if the numerical approximation to the vector field of interest is a nondecreasing function of each argument of the discrete approximation to the vector field.

or mixing organism substructures. Using Bolza-type objective functionals and backward reachability theory, we will leverage the insight above for constructing a theorem for solving the verification problem for such systems across local regions; then we will prescribe a scheme for aggregating the over-approximated backward reach-avoid tubes or sets (BRATs) of the respective subsystems across space-time.

Paper Goals: Our goal here is the verification of *complex* and *nonlinear* behavior of *multi-agent autonomous systems* that is robust against an *assumed worst-case disturbance*[2], and preserves local safety objectives *under global cohesion goals*. Within our broader aim, we limit the scope of this work to devising a scheme for separately computing the extremals of local payoffs of various subsystems over as large a range of target tubes as desired over a complex state space; we then prescribe the numerically robust Voronoi Implicit Interface method (VIIM) for aggregating such locally computed BRATs.

Natural Swarms as an Inspiration: To achieve this goal, we will leverage our understanding of flocking in natural swarms, particularly European starlings (*Sturnus vulgaris*), and rely on tools from level set methods [4, 17]. Applications of the principles described herein may include the verification of cyber-physical systems or CPS, multi-agent robotic systems requiring dynamical dexterity [18], or dynamical systems with locally valid asymptotic controllers that do not admit a continuous control law for arriving at a globally asymptotically stable solution [19, Theorem II]. Mostly, we will work locally in our formulations, but occasionally will make global remarks.

Natural swarms provide clues on efficiently constructing a game's outcome, Hamiltonian, and hence control laws, and strategies that govern the transient behaviors of many systems that possess structural subsystems with the properties we have introduced in the foregoing. Through empirical [20–24] and theoretical findings [25], evidence now abounds that in certain natural species that exhibit collective behavior (see Fig. 1), convergence and group cohesion is based on simple topological interaction rules that they employ to keep a tab on one another in *local flocks* for collision avoidance, preserving density and structure in an anisotropic formation, and exhibiting flock splitting, vacuole, cordon, and flash expansion isotropically [26]. This aids these animals in emerging an eye-pleasing local anisotropic synchrony, which taken together among possibly hundreds of thousands of local interactions[3] [26], keep these animals whirling, swooping, and flying in isotropic formations [20]. Thus, individual agents aggregate into finite flocks, and flock motion is synergized via local topological interactions in order to realize a stable global heading and cohesion [25]. There exists evidence that when an individual within a flock of starlings senses danger (e.g. an attack from a Peregrine Falcon), it changes its course immediately. Owing to the lateral vision in such animals, immediate *nearest neighbors* change course in response. This information is propagated across the entire group of flocks within the fraction of a second [20], resulting in elegant formations cf. Fig. 1.

[2] We have ongoing work that will learn the worst-case disturbance under an H_∞ norm bound on the system's transfer function.

[3] It has been reported that no birds fly together with greater coordination and complexity than European starlings, with murmurations counting upwards of 750,000 individual birds!

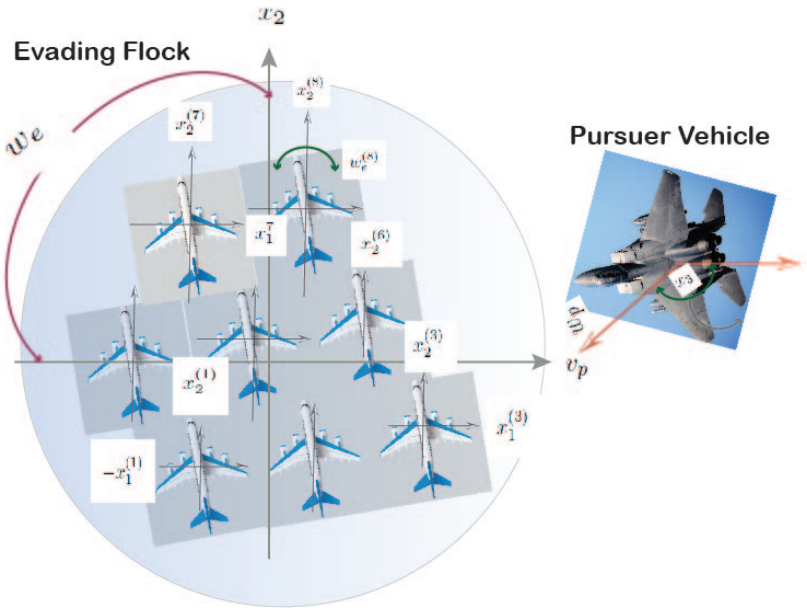

Fig. 2: Illustration of robust heading consensus for a flock with 8 aircraft. The evading player has all the evading agents under the will of its strategy. To every evading flock, there is at most one pursuing player.

While Jadbabaie et al. [25] introduced a graphical formulation based on a switched linear system to demonstrate that nearest neighbor rules cause agents to converge to the same heading, we stick with the nonlinear model of the system and employ *reachability analysis* as a verification tool. We introduce new insights, and computational techniques aimed at solving *practical* problems that cannot be otherwise analytically resolved nor numerically resolved without exploiting state substructures and parallelism. This work is the first to systematically provide a rational separated value function aggregation scheme on local state space substructures in computing *robustly controlled backward reach-avoid tubes (RCBRATs)* [3] for complex systems. The body of this paper goes thus: we introduce common notations and definitions in § 2; for readers not familiar with reachability theory and level set methods, we provide a background in Appendix A, and we encourage the pedestrian reader to get familiarized with the language by reading this appendix before continuing. Our proposed scheme is described in § 3; and we present results and insights from experiments in § 4. We conclude with remarks in § 5. Lastly, numerical results of our implementations and algorithm outlines are provided in the appendices.

2 Notations and Definitions.

Let us now introduce the notations that are commonly used in this article. Time variables e.g. t, t_0, τ, T will always be real numbers. We let $t_0 \leq t \leq t_f$ denote fixed, ordered

values of t. Vectors shall be column-wise stacked and be denoted by small bold-face letters i.e. $\mathbf{e}, \mathbf{u}, \mathbf{v}$ e.t.c. Matrices will be denoted by bold-math Latin upper case fonts e.g. $\mathbf{T}, \mathbf{S}$. Exceptions: the unit matrix is $\boldsymbol{I}$; and i, j, k, p are indices. Positive, negative, increasing, decreasing e.t.c. shall refer to strict corresponding property.

The set S of all $\boldsymbol{x}$ such that $\boldsymbol{x}$ belongs to the real numbers $\mathbb{R}$, and that $\boldsymbol{x}$ is positive shall be written as $S = \{\boldsymbol{x} \,|\, \boldsymbol{x} \in \mathbb{R}, \boldsymbol{x} > 0\}$. The cardinality of S shall be written as $[S]$. We define Ω as the open set in $\mathbb{R}^n$. To avoid the cumbersome phrase "the state $\boldsymbol{x}$ at time t", we will associate the pair $(\boldsymbol{x}, t)$ with the *phase* of the system for a state $\boldsymbol{x}$ at time t. Furthermore, we associate the Cartesian product of Ω and the space $T = \mathbb{R}^1$ of all time values as the *phase space*, $\Omega \times T$. The interior of Ω is denoted by $\text{int}\ \Omega$; whilst the closure of Ω is denoted $\bar{\Omega}$. We denote by $\delta\Omega\,(:= \bar{\Omega} \backslash \text{int}\ \Omega)$ the boundary of the set Ω.

Unless otherwise stated, vectors $\boldsymbol{u}(t)$ and $\boldsymbol{v}(t)$ are reserved for admissible control (resp. disturbance) at time t. We say $\boldsymbol{u}(t)$ (resp. $\boldsymbol{v}(t)$) is piecewise continuous in t, if for each t, $\boldsymbol{u} \in \mathcal{U}$ (resp. $\boldsymbol{v} \in \mathcal{V}$), $\mathcal{U}($ resp. $\mathcal{V})$ is a Lebesgue measurable and compact set. At all times, any of $\boldsymbol{u}$ or $\boldsymbol{v}$ will be under the influence of a *player* such that the motion of a state $\boldsymbol{x}$ will be influenced by the will of that player. Our operational domain involves conflicting objectives between various agents e.g. with a heading convergence goal under an external disturbance' influence. For agents that are members of a local coordination group, collision avoidance shall apply so that agents within a local neighborhood cooperate to avoid entropy and predatory pursuer(s). Thus, the problem at hand assumes that of a pursuit *game*. And by a game, we do not necessarily refer to a single game, but rather a *collection of games*. Such a game will terminate when *capture* occurs, that is the distance between players falls below a predetermined threshold.

Each player in a game shall constitute either a pursuer ($\boldsymbol{P}$) or an evader ($\boldsymbol{E}$). The cursory reader should not interpret $\boldsymbol{P}$ or $\boldsymbol{E}$ as controlling a single agent. In complex settings, we may have several pursuers (enemies) or evaders (peaceful citizens). However, when $\boldsymbol{P}$ or $\boldsymbol{E}$ governs the behavior of but one agent, these symbols will denote the agents themselves. Each evading agent, identified by its label i as a state superscript, is parameterized by three state components: its linear velocities $(\boldsymbol{x}_1^{(i)}, \boldsymbol{x}_2^{(i)})$, and its heading $w^{(i)}$. The state of an agent i within a flock F_j will be defined as $\boldsymbol{x}^{(i)_j}$ or $\boldsymbol{x}_j^i$.

Given the various possibilities of outcomes, the question of what is "best" will be resolved by a *payoff*, Φ, whose extremal over a time interval will constitute a *value*, $\boldsymbol{V}$[4]. We adopt Isaac's [27] language so that if the payoff for a game is finite, we shall have a *game of kind*; and for a game with a continuum of payoffs, we shall have *a game of degree*. The *strategy* executed by $\boldsymbol{P}$ or $\boldsymbol{E}$ during a game shall be denoted by $\alpha \in \mathcal{A}$ (resp. $\beta \in \mathcal{B}$). With this definition, a control law e.g. $\boldsymbol{u}^{(i)}$ played by a player e.g. $\boldsymbol{P}$ will affect *agent* i; and a collection of agents under $\boldsymbol{P}$'s *willpower* be referred to as a *flock*. We shall refer to an aggregation of flocks on a state space as a *murmuration* [5].

[4] The functional $\boldsymbol{\Phi}$ may be considered a functional mapping from an infinite-dimensional space to the space of real numbers.

[5] The definition of murmurations we use here has a semblance to the murmurations of possibly thousands of starlings observed in nature.

3 Methods.

We locally synthesize the kinematics of agents in a manner amenable to state representation by resolving local payoff extremals, $\{\boldsymbol{\Phi}_1, \cdots, \boldsymbol{\Phi}_{n_f}\}$. This is a state space partition induced by an aggregation of desired collective behavior from local flocks' values $\{\boldsymbol{V}_1, \cdots, \boldsymbol{V}_n\}$[6]. Suppose that the local control laws are properly coordinated, the region of the state space across which their coordinated influence might be exerted constitute a larger e.g. *manipulability volume* for a dexterous kinematic task. We now formalize definitions that will aid the modularization of the problem into manageable forms.

Definition 1 (Neighbors of an Agent). *We define the neighbors $\mathcal{N}_i(t)$ of agent i at time t as the set of all agents that lie within a predefined radius, r_i.*

Definition 2. *We define a flock, F, consisting of agents labeled $\{1, 2, \cdots, n_a\}$ as a collection of agents within a phase space $(\mathcal{X}, T)$ such that all agents within the flock interact with their nearest neighbors in a topological sense.*

Remark 1. Every agent within a flock has similar dynamics to that of its neighbor(s). Furthermore, agents travel at the same linear speed, v; the angular headings, w, however, may be different between agents, seeing we are dealing with a many-bodied system. Each agent's continuous-time dynamics, $\dot{\boldsymbol{x}}^{(i)}(t)$, evolves as

$$\begin{bmatrix} \dot{\boldsymbol{x}}_1^{(i)}(t) \\ \dot{\boldsymbol{x}}_2^{(i)}(t) \\ \dot{\boldsymbol{x}}_3^{(i)}(t) \end{bmatrix} = \begin{bmatrix} v(t)\cos \boldsymbol{x}_3^{(i)}(t) \\ v(t)\sin \boldsymbol{x}_3^{(i)}(t) \\ \langle w^{(i)}(t) \rangle_r \end{bmatrix}, \langle w^{(i)}(t) \rangle_r = \frac{1}{1+n_i(t)} \left(w^{(i)}(t) + \sum_{j \in \mathcal{N}_i(t)} w_j(t) \right) \tag{3.1}$$

for agents $i = \{1, 2, 3, ..., n_a\}$, where t is the continuous-time index, $n_i(t)$ is the number of agent i's neighbors at time t, $\mathcal{N}_i(t)$ denotes the sets of labels of agent i's neighbors at time t, and $\langle w^{(i)}(t) \rangle_r$ is the average orientation of agent i w.r.t its neighbors at time t. Note that for a game where all agents share the same constant linear speed and heading, (3.1) reduces to the dynamics of a Dubins vehicle in absolute coordinates with $-\pi \leq w^{(i)}(t) < \pi$. The averaging over the degrees of freedom of other agents in (3.1) is consistent with the *mean field theory*, whereby the effect of all other agents on any one agent is an approximation of a single averaged influence.

Definition 3 (Payoff of a Flock). *To every flock F_j (with a finite number of agents n_a) within a murmuration, $j = \{1, 2, \cdots, n_f\}$, we associate a payoff, $\boldsymbol{\Phi}_j$, that is the union of all respective agent's payoffs for expressing the outcome of a desired kinematic behavior.*

[6] Let the cursory reader understand that we use the concept of a flock loosely. The value function could represent a pallete of composed value functions whose extremals resolve local behaviors we would like to emerge over separated local regions of the state space of dextrous drone acrobatics [28], a robot balls juggling task [18] or any parallel task domain verification problem.

Assumptions: The many interacting subsystems under consideration employ (i) natural units of measurements that are the same for all agents; (ii) kinematics with same linear speeds but with a capacity for orientation changes; (iii) intra-flock agent interaction occurs within unique and distinct state space manifolds; and by agents maneuvering their direction, a kinematic alignment is obtained with other flocks; (iv) inter-flock interaction occurs when a pursuer is within a threshold of capturing any agent within the murmuration; (v) the interaction among respective flocks is described by the time-evolution of an interface, which is the zero-level set of the objective functional of the respective local flocks.

Given the recent results in robust numerical optimization of level sets of late, the last point is more of an axiom, than an assumption (see [29–32]). Viscosity solutions provide a particular means of finding a unique solution with a clear interpretation in terms of the generalized optimal control problem, even in the presence of stochastic perturbations. Each agent within a flock interacts with a fixed number of neighbors, n_c, within a fixed topological range, r_c. This topological range is consistent with findings in collective swarm behaviors and it reinforces *group cohesion* [20]. However, we are interested in *robust group cohesion* in reachability analysis. Therefore, we let a pursuer, $\boldsymbol{P}$, with a worst-possible disturbance attack the flock, and we take it that flocks of agents constitute an evading player, $\boldsymbol{E}$. Returning to (3.1), for a single flock, we now provide a sketch for the HJI formulation for a heading consensus problem.

3.1 Framework for Separated Payoffs

We now make the following assumptions to enable our problem formulation. Suppose that a murmuration's global heading is predetermined and each agent i within each flock, F_j, $(j = \{1, \cdots, n_f\})$ in the murmuration has a constant linear velocity, v^i. An agent's orientation is its control input, given by the average of its own orientation and that of its neighbors. Instead of metric distance interaction rules that make agents very vulnerable to predators [20], we resort to a topological interaction rule. With metric distance rules, we will have to formulate the breaking apart of value functions that encode a consensus heading problem in order to resolve the extrema of multiple payoffs; which is typically what we want to prevent in real-world autonomous tasks.

What constitutes an agent's neighbors are computed based on empirical findings and studies from the lateral vision of birds and fishes [20, 22, 25] that provide insights into their anisotropic kinematic density and structure. Importantly, starlings' lateral visual axes and their lack of a rear sector reinforces their lack of nearest neighbors in the front-rear direction. As such, this enables them to maintain a tight density and robust heading during formation and flight. The delineation of an agent's nearest neighbors is given in Algorithm 1. On lines 3 and 7 of Algorithm 1, cohesion is reinforced by leveraging the observations above. While the neighbor updates for an agent involve an $O(n^2)$ algorithm in Algorithm 1, we are merely dealing with $6-7$ agents at a time in a local flock – making the computational cost measly.

Each agent within a flock F_j interacts with a fixed number of neighbors, n_c, within a fixed topological range, r_c. The topological range can be set as the distance between the labels of agents in a flock. This topological range is consistent with findings in collective swarm behaviors and it reinforces *group cohesion* [20]. However, we are interested in

robust group cohesion in reachability analysis. Therefore, we let a pursuer, $\boldsymbol{P}$, with a worst-possible disturbance attack the flock, and we take it that flocks of agents constitute an evading player, $\boldsymbol{E}$.

3.2 Global Isotropy via Local Anisotropy

Structural anisotropy is not merely an effect of a preferential velocity in animal flocking kinematics but rather an explicit effect of the anisotropic interaction character itself: agents choose a mutual position on the state space in order to maximize the sensitivity to changes in heading and speed of neighbors as the neighbors' anisotropy is optimized via vision-based collision avoidance characteristically unrelated to the eye's structure [20].

To reinforce robust group cohesion in local flocks, we randomly simulate a pursuer $\boldsymbol{P}_j$ against an evading agent in every flock F_j so that one agent is always relative coordinates with $\boldsymbol{P}^j$. In this specialized case, the $\boldsymbol{E}$ and $\boldsymbol{P}$'s speeds and maximum turn radii are equal: if both players start the game with the same initial velocity and orientation, the relative equations of motion show that $\boldsymbol{E}$ can mimic $\boldsymbol{P}$'s strategy by forever keeping the starting radial separation. As such, the *barrier* is closed and *the central theme in this game of kind is to determine the surface* [33]. We defer a thorough analysis of the nature of the surface to a future work.

Owing to the high-dimensionality of the state space, we cannot resolve this barrier analytically, hence we resort to numerical approximation methods – in particular, we leverage a parallel Lax-Friedrichs integration scheme [8] which we implement in Cupy [34] in order to provide a *consistent* and *monotone* solution to the Hamiltonians of the flocks. The assembly in the large of these respective Hamiltonians, and hence numerically robust solutions to the variational backward reeachability problem is resolved with a Voronoi tesselation of the zero-level sets of the boundaries of the flocks.

Therefore, for an agent i within a flock with index j in a murmuration, the equations of motion under attack from a predator p (see Fig. 2) in relative coordinates is

$$\begin{bmatrix} \dot{\boldsymbol{x}}_1^{(i)_j}(t) \\ \dot{\boldsymbol{x}}_2^{(i)_j}(t) \\ \dot{\boldsymbol{x}}_3^{(i)_j}(t) \end{bmatrix} = \begin{bmatrix} -v_e^{(i)_j}(t) + v_p^{(j)} \cos \boldsymbol{x}_3^{(i)_j}(t) + \langle w_e^{(i)_j} \rangle_r \boldsymbol{x}_2^{(i)_j}(t) \\ v_p^{(i)_j}(t) \sin \boldsymbol{x}_3^{(i)_j}(t) - \langle w_e^{(i)_j} \rangle_r \boldsymbol{x}_1^{(i)_j}(t) \\ w_p^{(j)}(t) - \langle w_e^{(i)_j}(t) \rangle_r \end{bmatrix} \text{ for } i = 1, \cdots, n_a \tag{3.2}$$

where n_a is the number of agents within a flock, $\left(\boldsymbol{x}_1^{(i)_j}(t), \boldsymbol{x}_2^{(i)_j}(t)\right) \in \mathbb{R}^2$, and we have $\boldsymbol{x}_3^{(i)_j}(t) \in [-\pi, +\pi)$[7]. Read $\boldsymbol{x}_1^{(i)_j}(t)$: the first component of the state of an agent i at time t which belongs to the flock j in the murmuration at time t. In absolute coordinates, the equation of motion for *free agents* is

$$\begin{bmatrix} \dot{\boldsymbol{x}}_1^{(i)_j}(t) \\ \dot{\boldsymbol{x}}_2^{(i)_j}(t) \\ \dot{\boldsymbol{x}}_3^{(i)_j}(t) \end{bmatrix} = \begin{bmatrix} v_e^{(i)_j}(t) \cos \boldsymbol{x}_3^{(i)_j}(t) \\ v_e^{(i)_j}(t) \sin \boldsymbol{x}_3^{(i)_j}(t) \\ \langle w_e^{(i)_j}(t) \rangle_r \end{bmatrix}. \tag{3.3}$$

[7] We have multiplied the dynamics by -1 so that the extremal's resolution evolves backwards in time.

3.3 Flock Motion from Aggregated Value Functions

We introduce the union operator i.e. $\cup$ below as an aggregation symbol since the respective payoffs of each agent in a flock may be implicitly or explicitly constructed[8] – when it is implicitly represented, say from a signed distance function, we shall aggregate the payoff of agents 1 and 2 as

$$\cup\{\boldsymbol{\Phi}_1(\boldsymbol{x},t),\boldsymbol{\Phi}_2(\boldsymbol{x},t)\} \equiv \boldsymbol{\Phi}_1(\boldsymbol{x},t) \cup \boldsymbol{\Phi}_2(\boldsymbol{x},t) = \min(\boldsymbol{\Phi}_1(\boldsymbol{x},t),\boldsymbol{\Phi}_2(\boldsymbol{x},t)) \tag{3.4}$$

otherwise, other appropriate arithmetic or logical operation shall apply.

We assume that the *value* of a flock heading control (differential game) exists. And by an extension of Hamilton's principle of least action, the terminal motion of a flock coincide with the extremal of the payoff functional

$$\boldsymbol{V}(\boldsymbol{x},t) = \inf_{\beta^{(1)}\in\mathcal{B}^{(1)}} \sup_{\boldsymbol{u^{(1)}}\in\mathcal{U}^{(1)}} g^{(1)}(\boldsymbol{x}(T)) \cup \cdots \inf_{\beta^{(n_f)}\in\mathcal{B}^{(n_f)}} \sup_{\boldsymbol{u}^{(n_f)}\in\mathcal{U}^{(n_f)}} g^{(n_f)}(\boldsymbol{x}(T))$$

where n_f is the total number of distinct flocks in a murmuration. The resolution of this equation admits a viscosity solution to the following variational terminal HJI PDE [2]

$$\cup_{j=1}^{n_f}\left[\cup_{i=1}^{n_a}\left(\frac{\partial \boldsymbol{V}_i}{\partial t}(\boldsymbol{x},t) + \min\left[0, \boldsymbol{H}^{(i)}(\boldsymbol{x}^{(i)}, \boldsymbol{V}_x(\boldsymbol{x},t))\right]\right)\right] = 0. \tag{3.5}$$

with Hamiltonian,

$$\boldsymbol{H}^{(i)}(t;\boldsymbol{x}^{(i)},\boldsymbol{u}^{(i)},\boldsymbol{v}^{(i)},p^{(i)}) = \max_{u^{(i)}\in\mathcal{U}^{(i)}} \min_{v^{(i)}\in\mathcal{V}^{(i)}} \langle f^{(i)}(t;\boldsymbol{x},\boldsymbol{u}^{(i)},\boldsymbol{v}^{(i)}), p^{(i)}\rangle. \tag{3.6}$$

In swarms' collective motion, when e.g. a Peregrine Falcon attacks, immediate nearest agents change direction almost instantaneously. And because of the interdependence of the orientations of individual agents with respect to one another, all other agents respond instantaneously. Thus, we only simulate a single attack against a flock within the murmuration to realize robust cohesion.

A pursuer can attack any flock within the murmuration from a distinct surface: a $\boldsymbol{P}$ direction: this side of the surface reached after penetration in the $\boldsymbol{P}-[\boldsymbol{E}-]$ direction is the $\boldsymbol{P}-[\boldsymbol{E}]$ *side* [27]. We attribute the term *in the small* to determine the smooth parts of the singular surface solution when a pursuer attacks, and when they are stitched together into the total solution, we shall describe them as *in the large*. There exists at least one value $\bar{\alpha}$ of α such that if $\alpha = \bar{\alpha}$, no vector in the β-vectogram[9] penetrates the surface in the E-direction. Similar arguments can be made for $\bar{\beta}$ which prevents penetration in the P-direction. We adopt [27]'s terminology and call these surfaces semi-permeable surfaces (SPS).

Throughout the game, we assume that the roles of $\boldsymbol{P}$ and $\boldsymbol{E}$ do not change, so that when capture can occur, a necessary condition to be satisfied by the saddle-point controls of the players is the Hamiltonian, $\boldsymbol{H}^i(\boldsymbol{x},p)$.

[8] In resolving the zero-level sets of HJ value functions, it is typical to represent the payoff's surface as the isocontour of some function (usually a signed distance function).

[9] A $\beta-$vectogram is the resulting state space when a the strategy β is applied in computing the optimal control law for an agent.

Theorem 1. *For a flock, F_j, the Hamiltonian is the total energy given by a summation of the exerted energy by each agent i so that we can write the main equation or total Hamiltonian of a murmuration as*

$$\boldsymbol{H}(\boldsymbol{x},p) = \max_{w_e^{(k)_j}\in[\underline{w}_e^j,\bar{w}_e^j]} \min_{w_p^{(k)_j}\in[\underline{w}_p^j,\bar{w}_p^j]} \cup_{j=1}^{n_f}\left[H_a^{(k)_j}(\boldsymbol{x},p)\cup\left(\cup_{i=1}^{n_a-1}H_f^{(i)_j}(\boldsymbol{x},p)\right)\right] \tag{3.7}$$

$$\begin{aligned}
&= \cup_{j=1}^{n_f}\Big(\cup_{i=1}^{n_a-1}\left[p_1^{(i)_j}\, v^{(i)_j}\cos\boldsymbol{x}_3 + p_2^{(i)_j}\, v^{(i)_j}\sin\boldsymbol{x}_3 + p_3^{(i)_j}\,\langle w_e^{(i)_j}\rangle_r\right] \\
&\quad\cup\Big[p_1^{(k)_j}\left(v^{(k)_j} - v^{(k)_j}\cos\boldsymbol{x}_3^{(k)_j}\right) - p_2^{(k)_j}v^{(k)_j}\sin\boldsymbol{x}_3^{(k)_j} - \underline{w}_p^j|p_3^{(k)_j}| \\
&\quad\quad + \bar{w}_e^j\left|p_2^{(k)_j}\boldsymbol{x}_1^{(k)_j} - p_1^{(k)_j}\boldsymbol{x}_2^{(k)_j} + p_3^{(k)_j}\right|\Big]\Big).
\end{aligned} \tag{3.8}$$

where $\boldsymbol{H}_a^{(k)_j}(\boldsymbol{x},p)$ is the Hamiltonian of the individual under attack by a pursuing agent, $\boldsymbol{P}$, and $H_f^{(i)_j}(\boldsymbol{x},p)$ are the respective Hamiltonians of the free agents, $i=\{1,\cdots,n_f\}$, within an evading flock in a murmuration, and not under the direct influence of capture or attack by $\boldsymbol{P}$; we denote by $w_e^{(i)_j}$ the heading of an evader i within a flock j and $w_p^{(j)}$ the heading of a pursuer aimed at flock j; $\underline{w}_e^{(k)_j}$ is the orientation that corresponds to the orientation of the agent with minimum turn radius among all the neighbors of agent k, inclusive of agent k at time t; similarly, $\bar{w}_e^{(k)_j}$ is the maximum orientation among all of the orientation of agent k's neighbors.

Corollary 1. *For the special case where the linear speeds of the evading agents and pursuer are equal i.e. $v_e^{(i)_j}(t) = v_p(t) = +1m/s$, we have the Hamiltonian as*

$$\begin{aligned}
\boldsymbol{H}(\boldsymbol{x},p) = \cup_{j=1}^{n_f}\Big(&\cup_{i=1}^{n_a-1}\left[p_1^{(i)_j}\,\cos\boldsymbol{x}_3 + p_2^{(i)_j}\,\sin\boldsymbol{x}_3 + p_3^{(i)_j}\,\langle w_e^{(i)_j}\rangle_r\right] \\
&\cup\Big[p_1^{(k)_j}\left(1-\cos\boldsymbol{x}_3^{(k)_j}\right) - p_2^{(k)_j}\sin\boldsymbol{x}_3^{(k)_j} - \underline{w}_p^j|p_3^{(k)_j}| \\
&+\bar{w}_e^j\left|p_2^{(k)_j}\boldsymbol{x}_1^{(k)_j} - p_1^{(k)_j}\boldsymbol{x}_2^{(k)_j} + p_3^{(k)_j}\right|\Big]\Big).
\end{aligned} \tag{3.9}$$

We adopt the essentially non-oscillatory Lax-Friedrichs scheme of [12, 13] in resolving (3.9). Denote by (x,y,z) a generic point in $\mathbb{R}^3$ so that given mesh sizes Δx, Δy, Δz, $\Delta t > 0$, letters u,v,w will represent functions on the x,y,z lattice $\Delta = \{(x_i,y_j,z_k) : i,j,k\in\mathbb{Z}\}$. We define the numerical monotone flux, $\hat{\boldsymbol{H}}^{(i)_j}(\cdot)$, of $\boldsymbol{H}_j^{(i)}(\cdot)$ as

$$\begin{aligned}
\hat{\boldsymbol{H}}^{(i)_j}(u^+,u^-,v^+,v^-,w^+,w^-) &= \boldsymbol{H}^{(i)_j}\left(\frac{u^+ + u^-}{2}, \frac{v^+ + v^-}{2}, \frac{w^+ + w^-}{2}\right) \\
&\quad -\frac{1}{2}\left[\alpha_x^{(i)_j}\left(u^+ - u^-\right) + \alpha_y^{(i)_j}\left(v^+ - v^-\right) + \alpha_z^{(i)_j}\left(w^+ - w^-\right)\right]
\end{aligned} \tag{3.10}$$

where

$$\alpha_x^{(i)_j} = \max_{\substack{a\leq u\leq b\\ c\leq v\leq d\\ e\leq w\leq f}} |\boldsymbol{H}_u^{(i)_j}(\cdot)|,\ \alpha_y^{(i)_j} = \max_{\substack{a\leq u\leq b\\ c\leq v\leq d\\ e\leq w\leq f}} |\boldsymbol{H}_v^{(i)_j}(\cdot)|,\ \alpha_z^{(i)_j} = \max_{\substack{a\leq u\leq b\\ c\leq v\leq d\\ e\leq w\leq f}} |\boldsymbol{H}_w^{(i)_j}(\cdot)| \tag{3.11}$$

are the dissipation coefficients, controlling the level of numerical viscosity in order to realize a stable solution that is physically realistic [12]. Here, the subscripts of $\boldsymbol{H}$ are the partial derivatives w.r.t the subscript variable, and the flux, $\hat{\boldsymbol{H}}(\cdot)$ is monotone for $a \leq u^{\pm} \leq b, c \leq v^{\pm} \leq d, e \leq w^{\pm} \leq f$. We adopt the total variation diminishing Runge-Kutta scheme of [35] in efficiently calculating essentially non-oscillating upwinding finite difference gradients of $\boldsymbol{H}(\cdot)$.

3.4 ComplexBRAT by Voronoi Tesselaton of Local ϵ-BRAT Interfaces

The method we propose here is inspired by the algorithmic notions of robust, self-organizing emergent "behaviors" where efficiency and consistency is important when considering the interconnection between moving interfaces [30]. In our case, the physics of the local interface of the flocks that constitute a murmuration possesses topological complexity arising from local value function boundaries that evolve temporally e.g. via intersection or destruction of interfaces as a result of physical phenomena changes such as vacuole, splitting, or flash expansion inherent in starlings murmurations (cf. Fig. 1).

Suppose that the boundaries between two flocks F_j, F_k is a closed hypersurface, moving through time i.e. $\Gamma_{jk}(t=0) \in \mathbb{R}^N$ with speed v_j as given in (A.7). We can solve the internally generated level set equation (A.7) to obtain the capture surface of respective flocks (see subsection 3.3). Given the value function aggregation scheme (cf. 3.5), we are interested in solving for the externally generated velocity field, v_{ext}, induced by a flock's kinematics in light of (3.2) so that v_j in (3.2) is now a parameter for every level set, instead of just the level set of the interface alone. We call v_{ext} the external velocity, so that at the zero level set, we have

$$v_{ext}^j = v_j \text{ when } \boldsymbol{V}_j = 0. \tag{3.12}$$

The key idea here is that we stitch the interfaces $\Gamma_{jk}, \Gamma_{kl}, \Gamma_{lm}$, by leveraging motion involving mean curvature [36, §4.1] in systems characterized by multi-phase kinetics. Therefore, a gradient descent on the energies of the respective flocks at the zero level set can be computed from

$$\cup_{i=1}^{n_f} \boldsymbol{V}_i = \sum_{j\neq k} \gamma_{jk} \Upsilon(\Gamma_{jk}),\ \text{ for } (j,k) \in \{i \mid i = 1, \cdots, n_f\} \text{ where } \boldsymbol{V}_i \in \Omega, \tag{3.13}$$

Υ is the area covered by the multi-flock interface, $\boldsymbol{V}_i \cap \boldsymbol{V}_j = (\partial \boldsymbol{V}_i) \cap (\partial \boldsymbol{V}_j)$ for $i \neq j$, $\boldsymbol{V}_i \cap \boldsymbol{V}_i = (\partial \boldsymbol{V}_i) \cap (\partial \boldsymbol{V}_i) \equiv \emptyset$. In addition, we require the surface tension, γ_{jk}, to be positive so that the interfaces shrink as the level set equation evolves over time; we do this by imposing the following triangle inequality $\gamma_{jk} + \gamma_{kl} \geq \gamma_{jl}$ for distinct j, k, l in order to assure that (3.13) is well-posed [31]. Where interacting flocks share a boundary,

we characterize such higher order junctions by triple hypersurfaces, by tracking the ϵ-BRATs for an $\epsilon > 0$. The kinematics of these ϵ-BRATs under attack by predators constitute the evolution of the event-driven behavior of murmurations that swoop, swirl, or whirl in order to evade capture (see Fig. 1).

The speed of the interface, at a point $\boldsymbol{x} \in \Gamma_{jk}$ a distance from a triple junction, is given by

$$v_N(\boldsymbol{x}) = \gamma_{jk}\mathcal{K}_{jk}(\boldsymbol{x}) \tag{3.14}$$

for a curvature $\mathcal{K}_{jk}(\boldsymbol{x}) = \mathcal{K}_{kj}(\boldsymbol{x})$, and a normal speed $v_N(\boldsymbol{x})$. We implicitly initialize the payoff, $\boldsymbol{\Phi}_j^i$ of each agent labeled $p \in \{1, \cdots n_a\}$ within every flock, F_j, $\forall\, j = 1, \cdots, n_f$ as a signed distance function $d_{\boldsymbol{\Phi}_j^i}(\boldsymbol{x})$ to a phase (set) in $\boldsymbol{\Phi}_j^i \in \Omega$ so that it yields an Euclidean distance to the boundary $\partial\boldsymbol{\Phi}_j^i$ whose sign bit is an indicator function, signifying that if a point $\boldsymbol{x} \in \mathbb{R}^n$ is inside or outside Σ i.e.

$$d_{\boldsymbol{\Phi}_j^i}(\boldsymbol{x}) = \begin{cases} \inf_{\boldsymbol{z}^{(i)} \in \partial\boldsymbol{\Phi}_j^i} \mid \boldsymbol{x} - \boldsymbol{z}^{(i)} \mid, & \boldsymbol{x} \in \boldsymbol{\Phi}_j^i, \\ -\inf_{\boldsymbol{z}^{(i)} \in \partial\boldsymbol{\Phi}_j^i} \mid \boldsymbol{x} - \boldsymbol{z}^{(i)} \mid, & \boldsymbol{x} \notin \boldsymbol{\Phi}_j^i, \end{cases} \tag{3.15}$$

so that each agent's initial position is uniquely represented on the overall vectogram based on the value of $\boldsymbol{z}^{(i)}$. In order to maintain a consistent level set representation for each payoff, (e.g. when flocks split, expand, or spread out, cf. Fig. 1), the structure of interface must be maintained as time evolves. We follow Adalsteinsson et. al's [29] construction and write the level set equation as

$$v_{ext}^j \cdot \nabla \boldsymbol{V}_j = 0, \;\; \text{where } v_{ext}^j = \frac{\nabla\boldsymbol{\Phi}}{|\nabla\boldsymbol{\Phi}|}, \tag{3.16}$$

so that the level set function $\boldsymbol{V}_j$ remains the signed distance function as time evolves. When the level set functions must be evolved concurrently, we reparameterize the level set equation with an unsigned distance function as a union of an $\epsilon > 0$ super-level sets of the respective flocks

$$\frac{\partial\boldsymbol{\Phi}}{\partial t}(\boldsymbol{x}, t) - \nabla \cdot v_{ext}^j \, |\nabla\boldsymbol{\Phi}(\boldsymbol{x}, t)| = \epsilon. \tag{3.17}$$

That is the level set corresponding to the interface is now a neighbor of nearby level sets; this makes the motion of the zero level set that corresponds to the interface (A.7) is surrounded by the motion of nearby level sets. Similar to [30], we define Voronoi interface Γ_V as the set of of all points $\boldsymbol{x}$ that are equidistant to at least two different ϵ-level sets belonging to different flocks, and no closer to any other ϵ-level set i.e.

$$\begin{aligned} \Gamma_V &= \{\boldsymbol{x} \in \Omega : \exists i \neq j\} \\ \text{such that } d(\boldsymbol{x}, \Gamma_{\epsilon,i}) &= d(\boldsymbol{x}, \Gamma_{\epsilon,j}) \leq d(\boldsymbol{x}, \Gamma_{\epsilon,k}) \, \forall\, k \neq i, j, \end{aligned} \tag{3.18}$$

where $\Gamma_{\epsilon,i}$ is the ϵ-level set corresponding to a flock i.

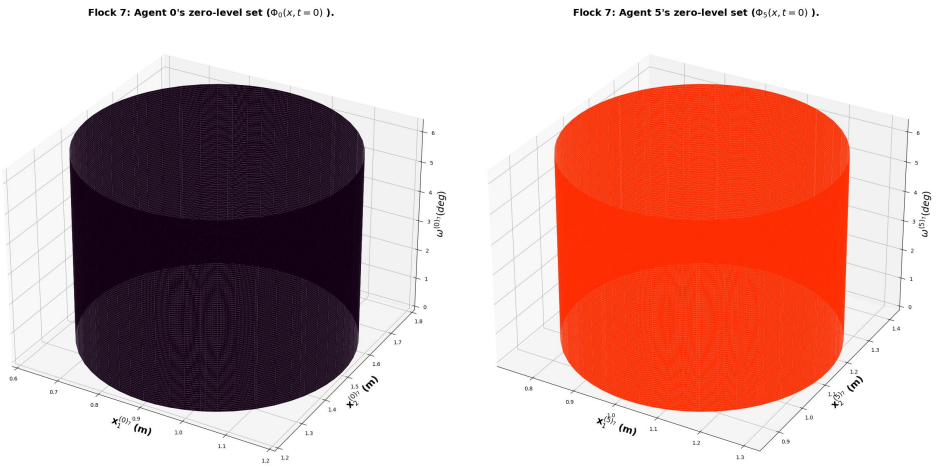

Fig. 3: Implicit representation of the payoffs for agents 2 and 5 within flock 7.

4 Experiments

At issue is a family of games with different target sets for local flocks that on the whole constitute a murmuration. Every agent's target position is initialized as

$$\rho_j \left[r_c \cos(\tfrac{i\pi}{4}), r_c \sin(\tfrac{i\pi}{4}), h + i\,\delta h \right]^T \; \forall\, i \in \{1, \cdots n_a\}, \forall\, j \in \{1, \cdots n_f\}. \tag{4.1}$$

Here, ρ_j is a scaling factor that ensures adequate *inter-flock separation* on a grid, h, δh are appropriately problem-dependent parameters, and r_c is a collision avoidance radius. The set of grid points for which the states of (4.1) is defined are those point set for which $d_{\boldsymbol{\Phi}^i_j}(\boldsymbol{x})$ is fixed and $\Omega = \{\text{all grid points}\}$. We set $d_{\boldsymbol{\Phi}^i_j}(\boldsymbol{x}) = \text{sgn}(\boldsymbol{V}^i_j(\boldsymbol{x}))$ for all $\boldsymbol{x} \in \Omega$. Fig. 3 denote the representation of the payoffs of certain agents that constitute a flock. They are constructed from the signed distance function from all points on the grid to an interface in the spirit of the foregoing.

An adaptive allocation rule for robust cohesion lets $\boldsymbol{P}$ randomly aim against an agent within an evading flock in every iteration of the game (see Fig. 2) – since when hunting for a prey, an originally targeted prey may evade $\boldsymbol{P}$. The domain in which we calculate the BRT of the agent under attack in relative coordinates w.r.t a pursuer, and that of the other agents (within a flock) in absolute coordinates are respectively

$$\bar{\Omega}_{rel} = \mathbb{R}^2 \times \mathcal{S}^1, \quad \bar{\Omega}_{abs} = \{\cup_{p=1}^{n_a - 1} \bar{\Omega}^p_{abs} | \bar{\Omega}^p_{abs} \in \mathbb{R}^2 \times \mathcal{S}^1\}. \tag{4.2}$$

It follows that the domain that constitutes the BRAT for a flock F_j is

$$\bar{\Omega}^j_{flk} = \{\bar{\Omega}^j_{rel} \cup \bar{\Omega}^j_{abs}\}, \tag{4.3}$$

and the domain that constitutes the BRAT of a murmuration $F_j, \cdots, F_{n_f}$ is

$$\bar{\Omega}_{murmur} = \{\bar{\Omega}^j_{flk} \cup \bar{\Omega}^{j+1}_{flk} \cup \cdots \cup \bar{\Omega}^{n_f}_{flk}\}. \tag{4.4}$$

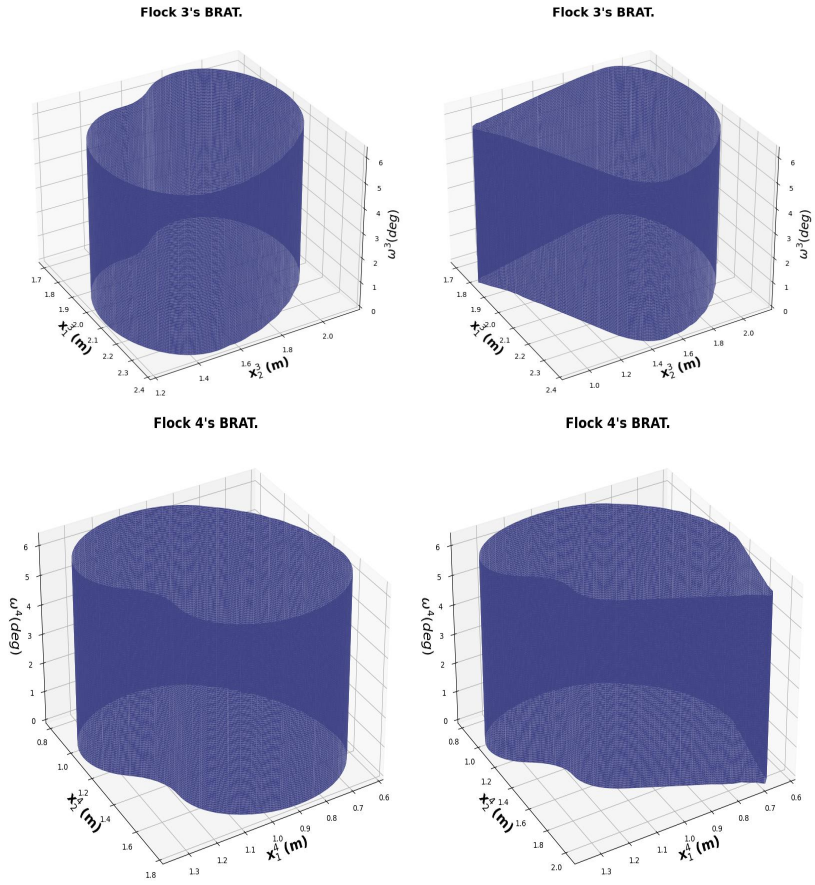

Fig. 4: Left: Interface or zero-level set for two example flocks. Right: Interfaces (zero-level set) of the evading flocks under attack from a pursuer at the end of the respective Lax-Friedrichs' integration scheme. Metric reach radius=$0.2m$, avoid Radius=$0.2m$. More results are included in Appendix D.

Since the orientations of neighboring agents are averaged throughout a flock, the information is inevitably propagated across the entire flock. Note that the above equations imply that the cardinality of all agents within a flock is $[n_a]$ and the cardinality of all agents within a murmuration is $[n_f]$. We define the payoff for a flock F_j as the union of the payoff of every individual agent that constitute it (that is, it is the union of the respective payoffs as shown in Fig. 3) i.e.

$$\boldsymbol{\Phi}_j = \boldsymbol{\Phi}_1 \cup \boldsymbol{\Phi}_2 \cup \cdots \cup \boldsymbol{\Phi}_{n_a-1} \cup \boldsymbol{\Phi}_{n_a}, \tag{4.5}$$

where a $\boldsymbol{\Phi}$ solves the level set PDE [4] in the form of the *unsigned distance function* of (3.17). The backward reach-avoid tubes we aim to compute constitute the states' set

from which the pursuer can drive the evader into the target set

$$\mathcal{L}_0 = \left\{ \boldsymbol{x} \in \bar{\Omega} | \left(\sqrt{\boldsymbol{x}_1^{(1)2} + \boldsymbol{x}_2^{(1)2}} - r_c^{(1)} \right) \cup \left(\sqrt{\boldsymbol{x}_1^{(2)2} + \boldsymbol{x}_2^{(2)2}} - r_c^{(2)} \right) \cup \cdots \right.$$
$$\left. \cup \left(\sqrt{\boldsymbol{x}_1^{(n_a)2} + \boldsymbol{x}_2^{(n_a)2}} - r_c^{(n_a)} \right) \right\} \tag{4.6}$$

where superscripts in parentheses denote the label of an agent, so that in a 3-D, $\mathcal{L}_0$ is akin to an uneven cylinder (see left inset of Fig. 4). The interface is the union of the zero-level set of the payoffs of the individual agents that constitute the flock (see Fig. 3). Each flock's zero-level set is distinct because the target set of its agents belong to unique positions in the state space.

Results from the numerical integration of the level set equation for different flocks is depicted in Fig. 4, and more results for other flocks are included in the Appendix D. Let us enquire. **Observe**: (a) Each flock's RCBRAT' surface is nonconvex; (b) The Lax-Friedrich's numerical integration scheme of the respective Hamilton-Jacobi value functions has discontinuities in the solution despite the value function being initially smooth; (c) Owing to the possibility of non-unique solutions to each initial value problem, the weighted essentially nonoscillatory entropy scheme we adopted helps in picking out "physically" relevant solutions to (3.8).

5 Conclusion

We have proposed an Hamilton-Jacobi-Isaacs systems verification scheme, based on Hamilton-Jacobi's reachability theory for constructing backward reachable tubes for a complex system with structural local behaviors that is characterized by topological nearest neighbor rules. These local spatio-temporal dynamics whose local interactions constitute a collective behavior. Using the key idea that the total energy within every subsystem is an aggregate of the respective energies of its individual agents, we have formulated a theorem for constructing the local Hamiltonians as well as value functionals.

Under the assumptions that we have (i) constant linear velocity among agents; (ii) each agent's orientation serves as the control input; (iii) intra-flock agent interaction occurs within unique and distinct state space manifolds; and by agents maneuvering their direction, a kinematic alignment is obtained with other flocks; and (iv) inter-flock interaction occurs when a pursuer is within a threshold of capturing any agent within the murmuration, we have presented a numerical input/state-constraint preserving scheme utilizing a time-constrained HJI formulation in a backward reachability setting.

References

1. Mitchell, I.: Games of two identical vehicles. Dept. Aeronautics and Astronautics, Stanford Univ. (July), 1–29 (2001) 1, 19
2. Mitchell, I.M., Bayen, A.M., Tomlin, C.J.: A time-dependent Hamilton-Jacobi formulation of reachable sets for continuous dynamic games. IEEE Transactions on Automatic Control **50**(7), 947–957 (2005). DOI 10.1109/TAC.2005.851439 1, 2, 9, 19, 20
3. Mitchell, I.: A Robust Controlled Backward Reach Tube with (Almost) Analytic Solution for Two Dubins Cars. EPiC Series in Computing **74**, 242–258 (2020) 1, 2, 4
4. Sethian, J.A.: Level Set Methods And Fast Marching Methods: Evolving Interfaces In Computational Geometry, Fluid Mechanics, Computer Vision, And Materials Science. Robotica **18**(1), 89–92 (2000) 1, 3, 14, 19
5. Evans, L., Souganidis, P.E.: Differential Games And Representation Formulas For Solutions Of Hamilton-Jacobi-Isaacs Equations. Indiana Univ. Math. J **33**(5), 773–797 (1984) 1, 2, 18, 19
6. Crandall, M.G., Lions, P.L.: Viscosity solutions of hamilton-jacobi equations. Transactions of the American mathematical society **277**(1), 1–42 (1983) 1, 2, 18, 19
7. Lions, P.L.: Generalized solutions of Hamilton-Jacobi equations, vol. 69. London Pitman (1982) 1
8. Crandall, M.G., Evans, L.C., Lions, P.L.: Some Properties of Viscosity Solutions of Hamilton-Jacobi Equations. Transactions of the American Mathematical Society **282**(2), 487 (1984) 1, 2, 8
9. Lygeros, J.: On reachability and minimum cost optimal control. Automatica **40**(6), 917–927 (2004) 2
10. Evans, L., Souganidis, P.E.: Differential games and representation formulas for solutions of Hamilton-Jacobi-Isaacs equations. Indiana Univ. Math. J **33**(5), 773–797 (1984) 2, 18, 19
11. Crandall, M.G., Majda, A.: Monotone Difference Approximations For Scalar Conservation Laws. Mathematics of Computation **34**(149), 1–21 (1980) 2
12. Crandall, M.G., Lions, P.L.: Two Approximations of Solutions of Hamilton-Jacobi Equations. Mathematics of Computation **43**(167), 1 (1984) 2, 10, 11
13. Osher, S., Shu, C.W.: High-Order Essentially Nonoscillatory Schemes for Hamilton-Jacobi Equations. SIAM Journal of Numerical Analysis **28**(4), 907–922 (1991) 2, 10
14. Herbert, S., Choi, J.J., Sanjeev, S., Gibson, M., Sreenath, K., Tomlin, C.J.: Scalable learning of safety guarantees for autonomous systems using hamilton-jacobi reachability. arXiv preprint arXiv:2101.05916 (2021) 2
15. Bajcsy, A., Bansal, S., Bronstein, E., Tolani, V., Tomlin, C.J.: An Efficient Reachability-based Framework for Provably Safe Autonomous Navigation in Unknown Environments. In: 2019 IEEE 58th Conference on Decision and Control (CDC), pp. 1758–1765. IEEE (2019) 2
16. Bansal, S., Tomlin, C.J.: DeepReach: A Deep Learning Approach to High-Dimensional Reachability 2
17. Osher, S., Sethian, J.A.: Fronts propagating with curvature-dependent speed: Algorithms based on hamilton-jacobi formulations. Journal of computational physics **79**(1), 12–49 (1988) 3
18. Burridge, R R and Rizzi, A A and Koditschek, D E: Sequential Composition of Dynamically Dexterous Robot Behaviors. Tech. Rep. 6 (1999) 3, 6
19. Brockett, R.W.: Asymptotic Stability and Feedback Stabilization. Differential Geometric Control Theory **27**(1), 181–191 (1983) 3
20. Ballerini, M., Cabibbo, N., Candelier, R., Cavagna, A., Cisbani, E., Giardina, I., Lecomte, V., Orlandi, A., Parisi, G., Procaccini, A., Viale, M., Zdravkovic, V.: interaction Ruling Animal Collective Behavior Depends On Topological Rather Than Metric Distance: Evidence From

A Field Study. Proceedings of the National Academy of Sciences **105**(4), 1232–1237 (2008). DOI 10.1073/pnas.0711437105. URL https://www.pnas.org/content/105/4/1232 3, 7, 8
21. Cavagna, A., Cimarelli, A., Giardina, I., Parisi, G., Santagati, R., Stefanini, F., Viale, M.: Scale-ffee correlations in starling flocks. Proceedings of the National Academy of Sciences **107**(26), 11,865–11,870 (2010) 3
22. Helbing, D., Farkas, I., Vicsek, T.: Simulating dynamical features of escape panic. Nature **407**(6803), 487–490 (2000) 3, 7
23. Vicsek, T., Czirók, A., Ben-Jacob, E., Cohen, I., Shochet, O.: Novel type of phase transition in a system of self-driven particles. Physical review letters **75**(6), 1226 (1995) 3
24. Bialek, W., Cavagna, A., Giardina, I., Mora, T., Silvestri, E., Viale, M., Walczak, A.M.: Statistical mechanics for natural flocks of birds. Proceedings of the National Academy of Sciences **109**(13), 4786–4791 (2012) 3
25. Jadbabaie, A., Lin, J., Morse, A.S.: Coordination of groups of mobile autonomous agents using nearest neighbor rules. IEEE Transactions on automatic control **48**(6), 988–1001 (2003) 3, 4, 7
26. Haiken, M.: These birds flock in mesmerizing swarms of thousandsbut why is still a mystery. (2021). URL https://www.nationalgeographic.com/animals/article/these-birds-flock-in-mesmerizing-swarms-why-is-still-a-mystery 3
27. Isaacs, R.: Differential games: A mathematical theory with applications to warfare and pursuit, control and optimization. Kreiger, Huntigton, NY (1965) 5, 9, 18
28. Kaufmann, E., Loquercio, A., Ranftl, R., Müller, M., Koltun, V., Scaramuzza, D.: Deep Drone Acrobatics. arXiv preprint arXiv:2006.05768 (2020) 6
29. Adalsteinsson, D., Sethian, J.A.: The Fast Construction Of Extension Velocities In Level Set Methods. Journal of Computational Physics **148**, 2–22 (1999) 7, 12
30. Saye, R.I., Sethian, J.A.: The Voronoi Implicit Interface Method for Computing Multiphase Physics. Proceedings of the National Academy of Sciences of the United States of America **108**(49), 19,498–19,503 (2011) 7, 11, 12
31. Zaitzeff, A., Esedoglu, S., Garikipati, K.: On the voronoi implicit interface method. SIAM Journal on Scientific Computing **41**(4), A2407–A2429 (2019) 7, 11
32. Karnakov, P., Litvinov, S., Koumoutsakos, P.: Computing Foaming Flows Across Scales: From Breaking Waves to Microfluidics. arXiv preprint arXiv:2103.01513 (2021) 7
33. Merz, A.: The game of two identical cars. Journal of Optimization Theory and Applications **9**(5), 324–343 (1972) 8, 18, 21
34. Nishino, R., Loomis, C., Hido, S.: Cupy: A numpy-compatible library for nvidia gpu calculations. 31st confernce on neural information processing systems **151** (2017) 8
35. Osher, S., Shu, C.W.: Efficient Implementation of Essentially Non-Oscillatory Shock Capturing Schemes. Tech. rep., NASA Langley Research Center, Hampton, Virginia (1987) 11
36. Osher, S., Fedkiw, R.: Level Set Methods and Dynamic Implicit Surfaces. Applied Mechanics Reviews **57**(3), B15–B15 (2004) 11, 21
37. Sethian, J.A.: Numerical Methods for Propagating Fronts. In: Variational methods for free surface interfaces, pp. 155–164. Springer (1987) 19

A Reachability for Systems Verification.

A basic characteristic of a control system is to determine the point sets within the state space that are *reachable* with a control input choice. An example objective in *reachability analysis* could be a target ($\mathcal{L}$) protection objective by an evading player from a pursuing player. Our treatment here is a special case of Isaac's homicidal chauffeur's game [27], whereupon $\boldsymbol{P}$ and $\boldsymbol{E}$ travel at constant linear speeds but have different headings, e.g. where the $\boldsymbol{P}$ seeks to drive an evader, $\boldsymbol{E}$, into a target set ($\mathcal{L}_0$) or tube, $\mathcal{L}[[-T, 0], \mathcal{L}_0]$.

A.1 Backward Reachability from Differential Games Optimal Control

Backward reachability consists in avoiding an unsafe set of states under the worst-possible disturbance and at all times. The verification problem may consist in finding a *set of reachable states* that lie along the trajectories of the solution to a first order nonlinear P.D.E. that originates from some initial state $\boldsymbol{x}_0 = \boldsymbol{x}(0)$ up to a specified time bound, $t = t_f$: *from a set of initial and unsafe state sets, the time-bounded safety verification problem is to determine if there is an initial phase that the solution to the P.D.E. enters an unsafe set*. Backward reachable sets (BRS) or tubes (BRTs) are popularly analyzed as a game of two vehicles with non-stochastic dynamics [33]. Such BRTs possess discontinuity at cross-over points (which exist at edges) on the surface of the tube, and may be non-convex. In general, we seek for a *terminal payoff* $g(\cdot) : \mathbb{R}^n \to \mathbb{R}$ to satisfy

$$|g(\boldsymbol{x}(t))| \leq k, \quad |g(\boldsymbol{x}(t)) - g(\hat{\boldsymbol{x}(t)}) \,| \leq k|\boldsymbol{x}(t) - \hat{\boldsymbol{x}}(t) \,| \tag{A.1}$$

for constant k and all $T \leq t \leq 0$, $\hat{\boldsymbol{x}}$, $\boldsymbol{x} \in \mathbb{R}^n$, $\boldsymbol{u} \in \mathcal{U}$ and $\boldsymbol{v} \in \mathcal{V}$.

Now, suppose that a pursuer's mapping strategy (starting at t) is $\beta : \bar{\mathcal{U}}(t) \to \bar{\mathcal{V}}(t)$ provided for each $t \leq \tau \leq T$ and $\boldsymbol{u}(t), \hat{\boldsymbol{u}}(t) \in \bar{\mathcal{U}}(t)$; then $\boldsymbol{u}(\bar{t}) = \hat{\boldsymbol{u}}(\bar{t})$ a.e. on $t \leq \bar{t} \leq \tau$ implies $\beta[\boldsymbol{u}](\bar{t}) = \beta[\hat{\boldsymbol{u}}](\bar{t})$ a.e. on $t \leq \bar{t} \leq \tau$. Suppose further that the player $\boldsymbol{P}$ is controlling the strategy β and minimizing, while the player $\boldsymbol{E}$ is controlling its strategy, α, and maximizing. For any admissible control-disturbance pair $(\boldsymbol{u}(\cdot), \boldsymbol{v}(\cdot))$ and initial phase $(\boldsymbol{x}_0, t_0)$, Crandall [6] and Evan's [5] claim is that there exists a unique trajectory, $\boldsymbol{\xi}(t)$, the motion of the dynamical system, (A.3), passing through phase $(\boldsymbol{x}_0, t_0)$ under the action of control $\boldsymbol{u}$, and a worst-possible disturbance $\boldsymbol{v}$, and observed at a time t afterwards i.e.

$$\boldsymbol{\xi}(t) = \boldsymbol{\xi}(t; t_0, \boldsymbol{x}_0, \boldsymbol{u}(\cdot), \boldsymbol{v}(\cdot)). \tag{A.2}$$

Equation (A.2) is a solution of the following dynamical system, represented as a first-order p.d.e.

$$\dot{\boldsymbol{x}}(\tau) = f(\tau, \boldsymbol{x}(\tau), \boldsymbol{u}(\tau), \boldsymbol{v}(\tau)) \quad T \leq \tau \leq t, \quad \boldsymbol{x}(t) = \boldsymbol{x}, \tag{A.3}$$

almost everywhere (a.e.); where $f(\tau, \cdot, \cdot, \cdot)$ and $\boldsymbol{x}(\cdot)$ are bounded and Lipschitz continuous. This bounded Lipschitz continuity property assures uniqueness of the system response $\boldsymbol{x}(\cdot)$ to controls $\boldsymbol{u}(\cdot)$ and $\boldsymbol{v}(\cdot)$ [10]. a.e. with the property that

$$\boldsymbol{\xi}(t_0) = \boldsymbol{\xi}(t_0; t_0, \boldsymbol{x}_0, \boldsymbol{u}(\cdot), \boldsymbol{v}(\cdot)) = \boldsymbol{x}_0. \tag{A.4}$$

In backward reachability analysis, the lower value of the differential game [10] is used in constructing an analysis of the backward reachable set (or tube). The differential game's lower value for a solution $\boldsymbol{x}(t)$ that solves (A.3) for $\boldsymbol{u}(t)$ and $\boldsymbol{v}(t) = \beta[\boldsymbol{u}](\cdot)$ is used in backward reachability analysis, given as

$$\begin{aligned}\boldsymbol{V}^{-}(\boldsymbol{x},t) &= \inf_{\beta\in\mathcal{B}(t)} \sup_{\boldsymbol{u}\in\mathcal{U}(t)} \boldsymbol{\Phi}(\boldsymbol{u},\beta[\boldsymbol{u}]) \\ &= \inf_{\beta\in\mathcal{B}(t)} \sup_{\boldsymbol{u}\in\mathcal{U}(t)} \int_t^T l(\tau,\boldsymbol{x}(\tau),\boldsymbol{u}(\tau),\beta[\boldsymbol{u}](\tau))d\tau + g\left(\boldsymbol{x}(T)\right). \end{aligned} \tag{A.5}$$

Lemma 1 (Theorem 1, [2]). *The backward reachability problem resolves the infimum-supremum of the non-anticipative strategies of $\boldsymbol{P}$ and the controls of $\boldsymbol{E}$ as an extremum of the cost functional over a time interval (time of capture), $t \in [-T, 0]$ is given by*

$$\frac{\partial \boldsymbol{V}^{-}}{\partial t}(\boldsymbol{x},t) + \min\{0, \boldsymbol{H}^{-}(t;\boldsymbol{x},\boldsymbol{u},\boldsymbol{v},\boldsymbol{V}^{-}_{\boldsymbol{x}})\} = 0,\ \boldsymbol{x}\in\mathbb{R}^n, \tag{A.6a}$$

$$\boldsymbol{V}^{-}(\boldsymbol{x},0) = g(\boldsymbol{x}), \tag{A.6b}$$

$$\textit{where } \boldsymbol{H}^{-}(t;\boldsymbol{x},\boldsymbol{u},\boldsymbol{v},p) = \max_{u\in\mathcal{U}} \min_{v\in\mathcal{V}} \langle f(t;\boldsymbol{x},\boldsymbol{u},\boldsymbol{v}),p\rangle, \tag{A.6c}$$

and p, the co-state, is the spatial derivative of $\boldsymbol{V}^{-}$ w.r.t $\boldsymbol{x}$. where the vector field $\boldsymbol{V}^{-}_{\boldsymbol{x}}$ is known in terms of the game's terminal conditions so that the overall game is akin to a two-point boundary-value problem.

Henceforward, we will remove the negative superscript on the lower value and Hamiltonian (A.6).

Flock F_j and F_k within a murmuration, $F_j \cup F_k \cup F_l \cdots$ are separated by *partitions*, or *interfaces*, $\Gamma_{jk}, \Gamma_{kl}, \cdots$. This interface may be implicitly represented as a signed distance function $\boldsymbol{\Phi}(\boldsymbol{x})$ which is negative on the interior of each flock, and zero on the edges. The zero-level set (i.e. $\boldsymbol{\Phi}(\boldsymbol{x}) = 0$) corresponds to the interface $\boldsymbol{V}$ [37]. As the system evolves over time, F_j's interface (zero-level set) motion can be parameterized by time, so that the flow field $\boldsymbol{V}(\boldsymbol{x},t)$ is equivalent to the solution of the Cauchy-type Hamilton Jacobi partial differential equation [5, 6]:

$$\boldsymbol{V}_t + v_j|\nabla \boldsymbol{V}_j| = 0, \quad j = 1,\cdots,n_f, \tag{A.7}$$

where v_j is the flow speed for F_j. Equation (A.7) is the level set equation [4].

In the sentiment of [2], we say the zero sublevel set of $g(\cdot)$ in (A.6) i.e. $\mathcal{L}_0 = \{\boldsymbol{x} \in \bar{\Omega} \,|\, g(\boldsymbol{x}) \le 0\}$, is the *target set* in the phase space $\Omega \times \mathbb{R}$ for a backward reachability problem [1]. This target set[10] can represent the failure set, regions of danger, or obstacles to be avoided e.t.c. in the vectogram. And the *robustly controlled backward reachable tube* for $\tau \in [-T, 0]$[11] is the closure of the open set

$$\begin{aligned}\mathcal{L}([\tau,0],\mathcal{L}_0) = \{\boldsymbol{x}\in\Omega \,|\, &\exists\,\beta\in\bar{\mathcal{V}}(t)\,\forall\,\boldsymbol{u}\in\mathcal{U}(t), \exists\,\bar{t}\in[-T,0], \\ &\boldsymbol{\xi}(\bar{t})\in\mathcal{L}_0\}, \bar{t}\in[-T,0]\,. \end{aligned} \tag{A.8}$$

[10] Note that the target set, $\mathcal{L}_0$, is a closed subset of $\mathbb{R}^n$ and is in the closure of Ω.

[11] The (backward) horizon, $-T$ is negative for $T > 0$.

Read: the set of states from which the strategies β of $\boldsymbol{P}$, and for all controls $\mathcal{U}(t)$ of $\boldsymbol{E}$ imply that we reach the target set within the interval $[-T, 0]$. More specifically, following Lemma 2 of [2], the states in the reachable set admit the following properties w.r.t the value function $\boldsymbol{V}$

$$\boldsymbol{x} \in \mathcal{L}_0 \implies \boldsymbol{V}^-(\boldsymbol{x}, t) \leq 0 \text{ and } \boldsymbol{V}^-(\boldsymbol{x}, t) \leq 0 \implies \boldsymbol{x} \in \mathcal{L}_0. \tag{A.9}$$

B Nearest Neighbors of an Agent

Algorithm 1 Nearest Neighbors For Agents in a Flock.

Given a set of agents $\boldsymbol{a} = \{a_1, a_2, \cdots, a_{n_a} \mid [a] = n_a\}$ ▷ n_a agents in a flock F_k.
function UPDATENEIGHBOR(n)
    for i in $1, \ldots, n$ **do** ▷ Look to the right and update neighbors.
        for j in $i + 1, \ldots, n$ **do**
            COMPARE_NEIGHBOR($a[i]$, $a[j]$)
        end for
        for j in $i - 1$ down to 0 **do** ▷ Look to the left and update neighbors.
            COMPARE_NEIGHBOR($a[i]$, $a[j]$)
        end for
    end for
    for each $a_i \in F_k$, $i = 1, \cdots n_a$ **do** ▷ Recursively update agents' headings.
        Update headings according to (3.1).
    end for
end function

function COMPARE_NEIGHBOR(a_1, a_2) ▷ (a_1, a_2): distinct instances of AGENT.
    if $|a_1$.label - a_2.label$| < a_1.r_c^1$ ▷ r_c^n: agent n's capture radius, r_c.
        a_1.UPDATE_NEIGHBORS(a_2) **then**
    end if
end function

procedure AGENT(a_i, Neighbors={}) ▷ Neighbors: Set of neighbors of this agent.
        ▷ Agent a_i with attributes label $\in \mathbb{N}$, avoid and capture radii, r_a, r_c.
    function UPDATE_NEIGHBORS(neigh)
        if length(neigh)> 1 **then** ▷ Multiple neighbors.
            for each neighbor of neigh **do**
                UPDATE_NEIGHBORS(neighbor) ▷ Recursive updates.
            end for
        end if
        Add neigh to Neighbors
    end function
end procedure

C Hamiltonian of a Murmuration

In this appendix, we provide a derivation for the Hamiltonian of a flock, and by extension, that of a murmuration. In our implementations, the zero-level set is constructed implicitly from the isocontour of a signed distance function as described in [36, Chapter II].

Recall from (3.8) that the total Hamiltonian of a flock is a union of the mechanical energy of the free agents in a flock and the individual under attack i.e.

$$\boldsymbol{H}(\boldsymbol{x},p) = \max_{w_e^{(k)^j}\in[\underline{w}_e^j,\bar{w}_e^j]} \min_{w_p^{(k)^j}\in[\underline{w}_p^j,\bar{w}_p^j]} \cup_{j=1}^{n_f} \left[H_a^{(k)^j}(\boldsymbol{x},p) \cup \left(\cup_{i=1}^{n_a-1} H_f^{(i)^j}(\boldsymbol{x},p)\right)\right] \tag{C.1}$$

Proof of Theorem 1. We write the Hamiltonian of the free agents in absolute coordinates and the Hamiltonian of the agent under attack in relative coordinates with respect to the pursuer. A flock's Hamiltonian is Hamiltonian of the free agents is the aggregation of all the mechanical energy in the system in absolute coordinates i.e.

$$\cup_{i=1}^{n_a-1} H_f^{(i)^j}(\boldsymbol{x},p) = \cup_{i=1}^{n_a-1} \begin{bmatrix} p_1^{(i)^j} & p_3^{(i)^j} & p_3^{(i)^j} \end{bmatrix} \begin{bmatrix} v^{(i)^j}\cos \boldsymbol{x}_3 \\ v^{(i)^j}\sin \boldsymbol{x}_3 \\ \langle w_e^{(i)^j}\rangle_r \end{bmatrix} \tag{C.2}$$

where we have again dropped the time arguments for convenience. It follows that

$$\cup_{i=1}^{n_a-1} H_f^{(i)^j}(\boldsymbol{x},p) = \cup_{i=1}^{n_a-1} \left[p_1^{(i)^j}\, v^{(i)^j}\cos \boldsymbol{x}_3 + p_3^{(i)^j}\, v^{(i)^j}\sin \boldsymbol{x}_3 + p_3^{(i)^j}\, \langle w_e^{(i)^j}\rangle_r\right]. \tag{C.3}$$

Equation (3.8) can be re-written as

$$\boldsymbol{H}_a^{(k)^j}(\boldsymbol{x},p) = -\left(\max_{w_e^{(k)^j}\in[\underline{w}_e^j,\bar{w}_e^j]} \min_{w_p^{(k)^j}\in[\underline{w}_p^j,\bar{w}_p^j]} \begin{bmatrix} p_1^{(k)^j}(t)\; p_2^{(k)^j}(t)\; p_3^{(k)^j}(t) \end{bmatrix} \begin{bmatrix} -v_e^{(k)^j}(t) + v_p^{(j)}\cos \boldsymbol{x}_3^{(k)^j}(t) + \langle w_e^{(k)^j}\rangle_r(t)\boldsymbol{x}_2^{(k)^j}(t) \\ v_p^j(t)\sin \boldsymbol{x}_3^{(k)^j}(t) - \langle w_e^{(k)^j}\rangle_r(t)\boldsymbol{x}_1^{(k)^j}(t) \\ w_p^j(t) - \langle w_e^{(k)^j}(t)\rangle_r \end{bmatrix}\right), \tag{C.4}$$

where $p_l^{(k)^j}(t)\;|_{l=1,2,3}$ are the adjoint vectors [33]. For the pursuer, its minimum and maximum turn rates are fixed so that we have $\underline{w}_p^j$ as the minimum turn bound of the pursuing vehicle, and $\bar{w}_p^j$ is the maximum turn bound of the pursuing vehicle. Henceforth, we drop the templated time arguments for ease of readability. Rewriting (C.4), we find

that

$$\begin{aligned}
\boldsymbol{H}_a^{(k)_j}(\boldsymbol{x},p) &= -\left(\max_{w_e^{(k)_j}\in[\underline{w}_e^j,\bar{w}_e^j]}\min_{w_p^{(k)_j}\in[\underline{w}_p^j,\bar{w}_p^j]}\left[-p_1^{(k)_j}v_e^{(k)_j}+p_1^{(k)_j}v_p^j\cos\boldsymbol{x}_3^{(k)_j}\right.\right.\\
&\left.\left.+p_1^{(k)_j}\langle w_e^{(k)_j}\rangle_r\boldsymbol{x}_2^{(k)_j}+p_2^{(k)_j}v_p^j\sin\boldsymbol{x}_3^{(k)_j}-p_2^{(k)_j}\langle w_e^{(k)_j}\rangle_r\boldsymbol{x}_1^{(i)_j}+p_3^{(k)_j}\left(w_p^j-\langle w_e^{(k)}\rangle_r\right)\right]\right),\\
&= p_1^{(k)_j}\left(v_e^{(k)_j}-v_p^j\cos\boldsymbol{x}_3^{(k)_j}\right)-p_2^{(k)_j}v_p^j\sin\boldsymbol{x}_3^{(k)_j}\\
&+\left(\max_{\langle w_e^{(k)_j}\rangle_r\in[\underline{w}_e^j,\bar{w}_e^j]}\min_{w_p^j\in[\underline{w}_p^j,\bar{w}_p^j]}\left[\langle w_e^{(k)_j}\rangle_r\left(p_2^{(k)_j}\boldsymbol{x}_1^{(k)_j}-p_1^{(k)_j}\boldsymbol{x}_2^{(k)_j}+p_3^{(k)_j}\right)-p_3^{(k)_j}w_p^j\right]\right).
\end{aligned}\tag{C.5}$$

It follows that we have from (C.5) that

$$\begin{aligned}
\boldsymbol{H}_a^{(k)_j}(\boldsymbol{x},p) = p_1^{(k)_j}\left(v_e^{(k)_j}-v_p^j\cos\boldsymbol{x}_3^{(k)_j}\right)-p_2^{(k)_j}v_p^j\sin\boldsymbol{x}_3^{(k)_j}-\underline{w}_p^j|p_3^{(k)_j}|\\
+\bar{w}_e^j\left|p_2^{(k)_j}\boldsymbol{x}_1^{(k)_j}-p_1^{(k)_j}\boldsymbol{x}_2^{(k)_j}+p_3^{(k)_j}\right|
\end{aligned}\tag{C.6}$$

and that

$$\boldsymbol{H}_f^{(i)_j}(\boldsymbol{x},p) = \left[p_1^{(i)_j}v^{(i)_j}\cos\boldsymbol{x}_3+p_3^{(i)_j}v^{(i)_j}\sin\boldsymbol{x}_3+p_3^{(i)_j}\langle w_e^{(i)_j}\rangle_r\right].\tag{C.7}$$

A fortiori the main equation (3.8) becomes

$$\begin{aligned}
\boldsymbol{H}(\boldsymbol{x},p) = \cup_{j=1}^{n_f}\left(\cup_{i=1}^{n_a-1}\left[p_1^{(i)_j}v^{(i)_j}\cos\boldsymbol{x}_3+p_2^{(i)_j}v^{(i)_j}\sin\boldsymbol{x}_3+p_3^{(i)_j}\langle w_e^{(i)_j}\rangle_r\right]\right.\\
\cup\left[p_1^{(k)_j}\left(v^{(k)_j}-v^{(k)_j}\cos\boldsymbol{x}_3^{(k)_j}\right)-p_2^{(k)_j}v^{(k)_j}\sin\boldsymbol{x}_3^{(k)_j}-\underline{w}_p^j|p_3^{(k)_j}|\right.\\
\left.\left.+\bar{w}_e^j\left|p_2^{(k)_j}\boldsymbol{x}_1^{(k)_j}-p_1^{(k)_j}\boldsymbol{x}_2^{(k)_j}+p_3^{(k)_j}\right|\right]\right).
\end{aligned}\tag{C.8}$$

For the special case where the linear speeds of the evading agents and pursuer are equal i.e. $v_e^{(i)_j}(t) = v_p(t) = +1m/s$, we have a murmuration's Hamiltonian as

$$\begin{aligned}
\boldsymbol{H}(\boldsymbol{x},p) = \cup_{j=1}^{n_f}\left(\cup_{i=1}^{n_a-1}\left[p_1^{(i)_j}\cos\boldsymbol{x}_3+p_2^{(i)_j}\sin\boldsymbol{x}_3+p_3^{(i)_j}\langle w_e^{(i)_j}\rangle_r\right]\right.\\
\cup\left[p_1^{(k)_j}\left(1-\cos\boldsymbol{x}_3^{(k)_j}\right)-p_2^{(k)_j}\sin\boldsymbol{x}_3^{(k)_j}-\underline{w}_p^j|p_3^{(k)_j}|\right.\\
\left.\left.+\bar{w}_e^j\left|p_2^{(k)_j}\boldsymbol{x}_1^{(k)_j}-p_1^{(k)_j}\boldsymbol{x}_2^{(k)_j}+p_3^{(k)_j}\right|\right]\right).
\end{aligned}\tag{C.9}$$

□

D Flocks' Robustly Controllable BRATs

Note that the symmetry between non-consecutive flock labels e.g. flock 1 and flock 3's RCBRAT is because the we multiplied the initial position of a flock's state by -1.

E Acknowledgment

For early feedback on the ideas reported here, a rising vote of thanks to Sylvia Herbert and Ian Abraham of the Mechanical and Aerospace Department of UC San Diego and Yale University respectfully. Cyril Zhang of Microsoft Research, NYC was helpful with programming (code) parallelization across multiple graphical processing units.

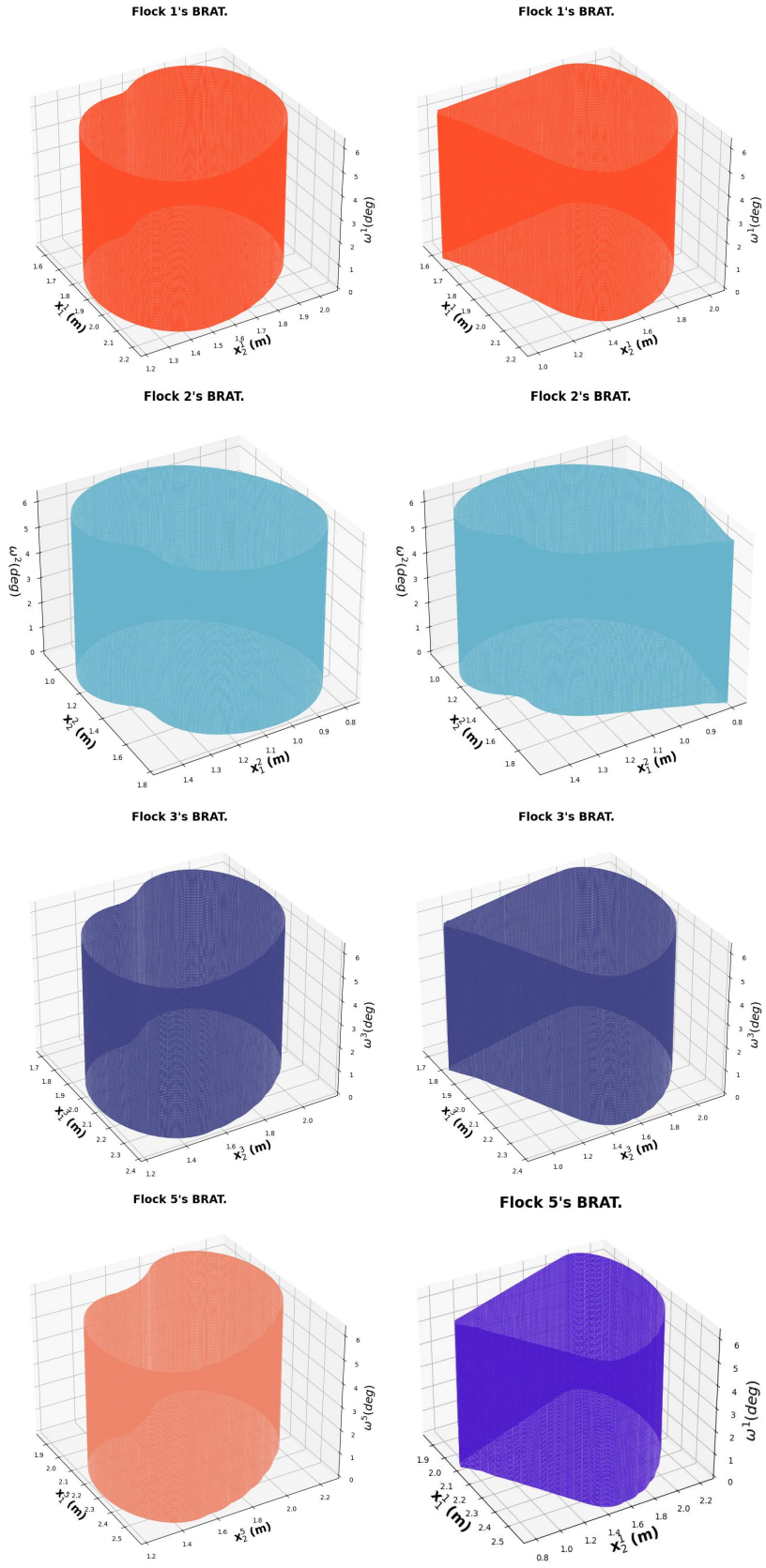

Fig. 5: Left: Initial zero-level set for various flocks at different initial conditions. Right: Evading flock's interface under a pursuer's attack after specific Lax-Friedrichs' integration. (Metric reach radius=$0.2m$, Avoid Radius=$0.2m$).